

Trichostatin A-mediated upregulation of p21^{WAF1} contributes to osteoclast apoptosis

TacGhee Yi^{1*}, Jeong-Hwa Baek^{1*},
Hye-Jin Kim¹, Mi-Hye Choi¹,
Sang-Beom Seo², Hyun-Mo Ryoo¹,
Gwan-Shik Kim¹ and Kyung Mi Woo^{1,3}

¹Department of Cell and Developmental Biology
Dental Research Institute and BK21 Program
School of Dentistry, Seoul National University
Seoul 110-749, Korea

²Department of Life Science
College of Natural Sciences, Chung-Ang University
Seoul 156-756, Korea

³Corresponding author: Tel, 82-2-740-8652;
Fax, 82-2-741-3193; E-mail, kmwoo@snu.ac.kr

*These authors contributed equally to this work.

Accepted 15 February 2005

Abbreviations: BMC, bone marrow cells; BMM, bone marrow derived macrophage; HDAC, histone deacetylase; HDI, histone deacetylase inhibitor; M-CSF, macrophage-colony stimulating factor; RANKL, receptor activator of nuclear factor κ B ligand; RNAi, RNA interference; TRAP, tartrate-resistant acid phosphatase; TSA, trichostatin A; μ CT, microcomputed tomography

Abstract

Histone deacetylase inhibitors (HDIs), a new class of anti-cancer agents, have been reported to suppress formation of osteoclast precursors and their fusion into multinucleated cells. However, little is known about the effect of HDIs on mature osteoclasts, which may have significance for their therapeutic use. Here, we demonstrate a novel action of HDIs on osteoclast apoptosis. Primary multinucleated mature osteoclasts were prepared from mouse bone marrow cells. Treatment of osteoclasts with the HDI trichostatin A (TSA) caused apoptosis, as confirmed by annexin V staining and caspase activation. TSA caused the upregulation of p21^{WAF1} in osteoclasts. To understand the role of p21^{WAF1} upregulation in TSA-treated osteoclasts, shRNA against p21^{WAF1}-containing lentivirus was introduced into osteoclasts. The suppression of p21^{WAF1} decreased TSA-directed osteoclast apoptosis. Collectively, our results provide evidence that TSA causes osteoclast apoptosis, which involves, in part, TSA-induced upregulation of

p21^{WAF1}, and strongly supports HDIs as potential therapeutic agents for excessive bone resorption.

Keywords: apoptosis; CDKN1A protein, mouse; cyclin-dependent kinase inhibitor p21; histone deacetylases; osteoclasts; RNA interference; trichostatin A

Introduction

Osteoporosis and inflammation- and tumor-induced bone destruction are pathologic conditions with excessive bone resorption caused by osteoclasts. Osteoclasts are derived from hematopoietic cells of monocyte/macrophage lineage, and differentiated in a specialized microenvironment of bone. Osteoclast precursor cells that express the receptor activator of nuclear factor κ B (RANK) on their cell surface can be differentiated into multinucleated osteoclasts by the RANK ligand (RANKL) presented by osteoblasts, stromal cells, and T-cells in the environment of the bone (Boyle *et al.*, 2003). Osteoclasts perform bone resorption and ultimately undergo apoptosis. The promotion of osteoclast apoptosis has become a very important therapeutic target for conditions involving excessive bone resorption (Weinstein and Manolagas, 2000). Physiological regulators and therapeutic agents, such as estrogen and bisphosphonates, effectively inhibit bone resorption by promoting osteoclast apoptosis (Hughes *et al.*, 1996; Luckman *et al.*, 1998).

Histone deacetylase inhibitors (HDIs) are a new promising class of anticancer agents, some of which are in clinical trials (Marks *et al.*, 2000; Piekarczyk and Bates, 2004). Chromatin structure, which can be modulated by the acetylation of histones, plays a role in gene expression (Wolffe and Hayes, 1999): the accumulation of acetylated histones is associated with a neutralization of the positive charge of lysine-residue, leading to an alteration in chromatin conformation. This may provide transcriptional factor complexes with greater access to the promoter regions of genes. The acetylation status of histones is determined by the activities of histone acetyltransferases and histone deacetylases (HDACs). Inhibition of HDAC activity by a number of structurally divergent classes of HDIs leads to hyperacetylation of histone. HDIs have been shown to induce growth arrest, differentiation, and/or apoptosis of proliferating cancer cells (Marks *et al.*, 2000; Piekarczyk and Bates, 2004). These effects of

HDIs are reported to be more pronounced in cancer cells than in normal cells; however, their mechanisms are unclear. p21^{waf1} is one of the best-studied genes whose expression is increased by HDIs in several types of cells (Marks *et al.*, 2000; Piekarczyk and Bates, 2004). HDI-induced activation of p21^{waf1} involves changes in promoter-associated proteins including HDAC1 (Gui *et al.*, 2004). p21^{waf1} is a well-known cyclin-dependent kinase inhibitor (CKI). This CKI can induce growth arrest and is also involved in differentiation and can modulate cell apoptosis (Coqueret, 2003). p21^{waf1} has also been suggested to play a role during osteoclast differentiation (Okahashi *et al.*, 2001; Sankar *et al.*, 2004).

Recently, HDIs have been reported to suppress osteoclastogenesis, suggesting a potential use for HDIs in treating bone diseases (Rahman *et al.*, 2003; Nakamura *et al.*, 2005). It has been reported that HDIs inhibit the formation of osteoclast precursor cells from bone marrow cells (BMCs) and suppress the fusion of osteoclast precursors into multinucleated cells. The inactivation of nuclear factor κ B and production of interferon- β have been demonstrated to underlie these effects (Rahman *et al.*, 2003; Nakamura *et al.*, 2005). Although HDI effects on mature osteoclasts may have therapeutic significance, little is known about these effects. This study examines the effect of HDI on mature osteoclasts. We report that the HDI trichostatin A (TSA) causes apoptosis of mature osteoclasts, and that TSA-induced upregulation of p21^{waf1} contributes to the apoptosis.

Materials and Methods

Reagents and antibodies

Recombinant human TGF- β 1, murine macrophage-colony stimulating factor (M-CSF), and human soluble RANKL were purchased from Peprotech (Cytolab, Rehovot, Israel). These cytokines were reconstituted in sterile water according to manufacturer's instructions. Trichostatin A and the Leukocyte Acid Phosphatase Stain Kit were from Sigma (St. Louis, MO). TSA was dissolved in absolute ethyl alcohol and stored at -20°C as a 1 mM stock solution. Cell culture reagents including α -MEM, FBS, and penicillin-streptomycin were from GibcoBRL (Gaithersburg, MD). West-Zol was from Intron Biotechnology (Seoul, Korea). AccuPower RT-Premix was from Bioneer (Daejeon, Korea). Anti-p21^{waf1}, anti-caspase 8, anti-actin, and HRP-conjugated IgG antibodies were obtained from Santa Cruz Biotechnology (Santa Cruz, CA). Anti-caspase 3 and anti-caspase 9 antibodies were from Cell Signaling Technology (Beverly, MA), and anti-p27^{KIP1} antibody

was from BD Pharmingen (Chicago, IL).

Cell culture

All procedures were approved by the Animal Subjects Office at Seoul National University, authorization number SNU-050503-9. Osteoclastogenesis from primary bone marrow cells (BMC) was induced as follows: nonadherent BMCs from 5-week-old female ICR mice (Samtaco, Umseong, Korea) were seeded at a density of 8×10^6 cells per 60-mm culture dish, 8×10^5 cells per well in 24-well plates, or 4×10^5 cells per well in 48-well plates and cultured in α -MEM with 10% FBS containing M-CSF (40 ng/ml) and TGF- β 1 (1 ng/ml). After one day, the cells were given fresh medium containing the same cytokines and cultured for an additional two days. These cells were used as bone marrow-derived macrophages (BMMs) (Fuller *et al.*, 2000). The BMMs were cultured for an additional four days in the presence of M-CSF (40 ng/ml) and soluble RANKL (100 ng/ml) to generate multinucleated osteoclasts. The culture medium was changed every day. In these cultures, tartrate-resistant acid phosphatase (TRAP)-positive multinucleated cells (MNCs) usually appeared 2 days after RANKL treatment. Osteoclast differentiation phenotypes were as reported previously (Yi *et al.*, 2006).

TRAP staining

At the end of the culture, cells in 48-well plates were stained for TRAP using a Leukocyte Acid Phosphatase Stain Kit (Sigma) according to the manufacturer's instructions. The numbers of TRAP-positive cells with three or more nuclei were counted under a light microscope.

Flow cytometry for apoptosis

BMCs seeded in a 24-well plate were cultured as above. Three days after the addition of M-CSF and RANKL, osteoclasts were treated with TSA for 18-20 h. Apoptotic cells were labeled using an Annexin V-FITC Apoptosis Detection Kit (BD Pharmingen, Chicago, IL). Analysis by flow cytometry using a FACS CaliburTM (BD Bioscience, San Diego, CA) was carried out within 1 h.

Extraction of total RNAs and semi-quantitative RT-PCR analysis

To evaluate mRNA expression, semi-quantitative RT-PCR was performed in a range of linear amplification. Total RNAs were isolated using easy-BlueTM RNA extraction reagent (Intron Biotechnology). Fifty μ l of first-strand cDNA was synthe-

sized from 1 μg of total RNA. One μl of cDNA was used for PCR amplification. The mouse primer sequences were as follows: p21^{WAF1}-forward (f), 5'-GTCCAATCCTGGTGATGTCC-3'; p21^{WAF1}-reverse (r), 5'-TCTGCGCTTGGAGTGATAGA-3'; p27^{KIP1}-f, 5'-AGAATAACCCGGGACTTGG-3'; p27^{KIP1}-r, 5'-TCTGACGAGTCAGGCATTTG-3'; GAPDH-f, 5'-TCA-CCATCTTCCAGGAGCG-3'; and GAPDH-r, 5'-CTG-CCTTACCACCTTCTTGA-3'.

Western blot analysis

Cell lysates were prepared using a buffer of 10 mM Tris-Cl, pH 7.5, 150 mM NaCl, 1 mM EDTA, pH 8.0, 1% Triton X-100, 0.5% sodium deoxycholate, 0.1% SDS, 1 mM PMSF, and a complete protease inhibitor cocktail tablet. The samples containing equal amounts of protein, were subjected to SDS-PAGE, and then transferred onto a polyvinylidene difluoride membrane. The membrane was blocked with 5% nonfat dried milk and incubated with each antibody followed by incubation with HRP-conjugated secondary antibody. Luminescence was detected with an LAS1000 (Fuji, Tokyo, Japan).

Lentiviral shRNAs

To overcome the low-efficiency transfection of primary BMCs, we chose to use lentiviral shRNA infection. Target sense sequences for RNAi were as follows: sh-p21 for shRNA against p21^{WAF1}, 5'-AACGGTGGAACTTTGACTTCG-3'; sh-ctrl for shRNA against LacZ, 5'-GCTACACAAATCAGCGATTT-3'. Each shRNA construct was produced using a BLOCK-iTTM U6 RNAi Entry Vector Kit (Invitrogen, Carlsbad, CA). The shRNA-expressing lentiviral constructs were generated using the BLOCK-iTTM Lentiviral RNAi Expression System (Invitrogen). Each lentiviral shRNA construct was introduced into the 293FT cell line and viral supernatants were collected and harvested. Infection with the lentiviral shRNA constructs was performed either simultaneously with or 2 days after treatment with RANKL. No cytotoxicity was observed. Western blotting was carried out to evaluate gene knockdowns by the shRNA constructs.

In vivo mouse calvarial resorption analyses

Female ICR mice (5-week-old) were anesthetized with ketamin (10 mg/kg) and xylazine (1 mg/kg). Collagen sponges were soaked with RANKL (1 μg), and RANKL (1 μg) plus TSA (30 ng) in a 20 μl volume and placed in subcutaneous tissue above the center of the sagittal suture, as described previously (Kim *et al.*, 2006). Four animals in each group were used in this study. Two days after in-

sertion, the mice were sacrificed and the calvariae were fixed in 4% paraformaldehyde. Calvarial bone was examined by microcomputed tomography (μCT) (Skyscan 1072, Skyscan, Aartselaar, Belgium). After scanning, a cubical region (3 mm \times 3 mm \times 3 mm) covering the sagittal suture was selected and the bone volume was measured (TomoNT, Skyscan). After μCT scanning, the samples were decalcified in 13% EDTA, embedded in paraffin, and sectioned in 5- μm -thick slices. The sections were stained with H-E or for TRAP enzyme. From four mice in each group, TRAP (+) cells attached on bone surface

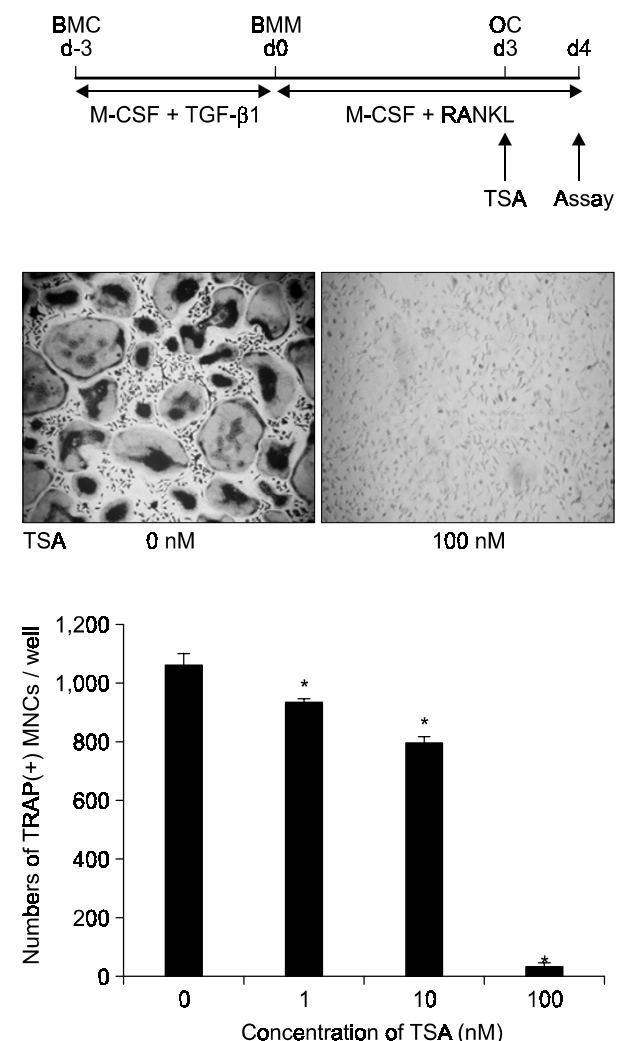


Figure 1. TSA treatment of osteoclasts reduces the number of TRAP-positive MNCs. BMMs were induced to differentiate to osteoclasts (OCs) by exposure to RANKL and M-CSF for 3 days. The osteoclasts were treated with TSA for 24 h in the presence of RANKL and M-CSF, followed by TRAP staining. TRAP-positive cells containing three or more nuclei were counted under the microscope. Representative images are presented. Data are averages \pm SDs ($n = 3$). *Statistically significant (Student's *t*-test, $P < 0.05$).

were counted in 4 mm-wide area along the sagittal suture in three different sections per mouse (total 12 sections per group) using Kappa Image Base Control 2.5 (KAPPA opto-electronics GmbH, Germany).

Statistical analysis

All *in vitro* experiments were performed in triplicate ($n = 3$) and repeated three times. All data are presented as averages \pm SDs. Statistical analysis was carried out using the Student's *t*-test.

Results

TSA causes osteoclast apoptosis

After TSA treatment, the multinucleated mature osteoclasts became detached from the culture dishes with remnants of TRAP-positive MNCs remaining on the

dishes. As shown in Figure 1, the number of TRAP-positive MNCs decreased profoundly with TSA treatment. Since 3-day-old cultures with RANKL produced substantial numbers of MNCs, this result strongly suggested that TSA might induce apoptosis of mature osteoclasts. This observation led us to determine whether mature osteoclasts undergo apoptotic cell death upon the exposure to TSA. After treatment with TSA for 18 h, the cells were collected and stained with Annexin V-FITC. Flow cytometry revealed that TSA substantially increased the cell population undergoing early apoptosis (Figure 2A). Next, we examined activation of caspases in TSA-treated osteoclasts. Western blot analysis showed that caspase 3 was clearly activated by TSA (Figure 2B). Cleavage of caspase 3 appeared after 6 h of TSA treatment in the time-course analysis. To discern the apoptotic pathways in detail, we examined activation of caspase 8 and caspase 9. Activation of

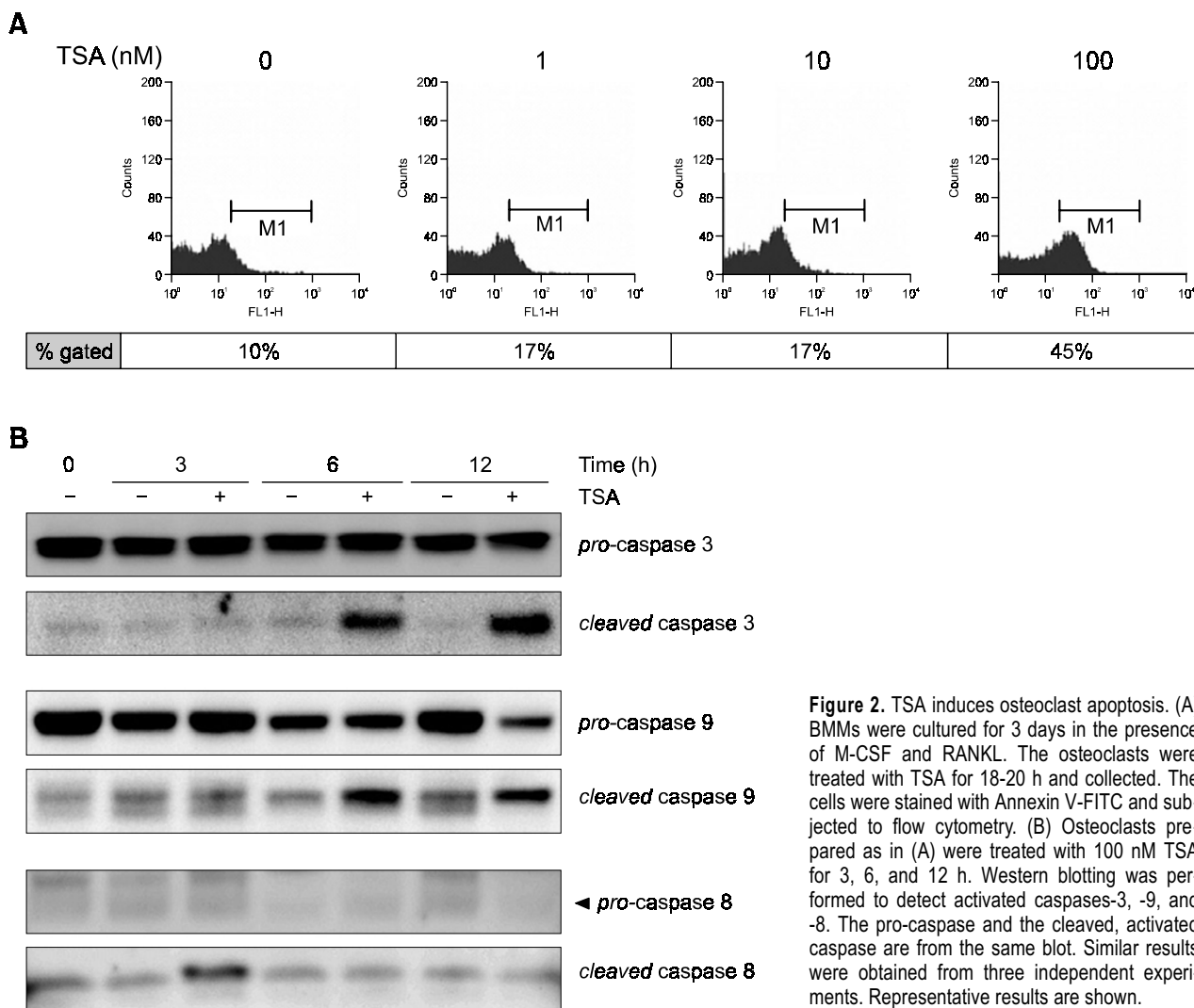


Figure 2. TSA induces osteoclast apoptosis. (A) BMMs were cultured for 3 days in the presence of M-CSF and RANKL. The osteoclasts were treated with TSA for 18-20 h and collected. The cells were stained with Annexin V-FITC and subjected to flow cytometry. (B) Osteoclasts prepared as in (A) were treated with 100 nM TSA for 3, 6, and 12 h. Western blotting was performed to detect activated caspases-3, -9, and -8. The pro-caspase and the cleaved, activated caspase are from the same blot. Similar results were obtained from three independent experiments. Representative results are shown.

caspace 9, but not caspace 8, appeared to occur along with cleavage of caspace 3, indicating that the pathway including caspases 9 and 3 may be involved in TSA-induced osteoclast apoptosis. Taken together, these results indicate that TSA causes osteoclast apoptosis.

TSA induces upregulation of p21^{WAF1} in osteoclasts

To understand the mechanism by which TSA induced osteoclast apoptosis, we examined TSA-induced alterations in the expression of several genes. Among these, the expression levels of p21^{WAF1} and p27^{KIP1} were examined, since p21^{WAF1} is induced by HDIs in several types of cells (Marks *et al.*, 2000; Gui *et al.*, 2004; Piekarz and Bates, 2004)

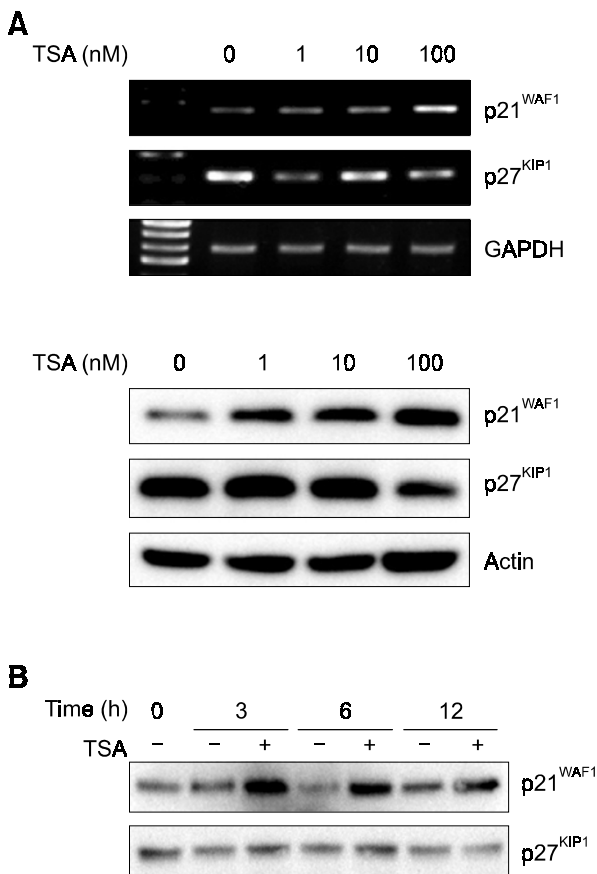


Figure 3. TSA causes upregulation of p21^{WAF1} in osteoclasts. (A) Osteoclast cultures, prepared as described above, were treated with TSA for 12 h. The expression levels of transcripts (upper panel) and proteins (lower panel) of p21^{WAF1} and p27^{KIP1} were analyzed by semi-quantitative RT-PCR and western blotting, respectively. GAPDH and actin served as loading controls for the RT-PCR and western blots, respectively. (B) Cultures were treated with 100 nM TSA for the indicated periods and p21^{WAF1} and p27^{KIP1} proteins were analyzed by western blotting. Similar results were obtained from three independent experiments. Representative results are shown.

and aberrant upregulation of p21^{WAF1} has been reported to occur during apoptosis (Gartel and Tyner, 2002; Liu *et al.*, 2003; Chopin *et al.*, 2004). Semi-quantitative RT-PCR and western blot analyses showed that upregulation of p21^{WAF1} was induced by TSA in a dose-dependent manner (Figure 3A). In a time-course analysis, upregulation of p21^{WAF1} appeared as early as 3 h after TSA treatment (Figure 3B). However, the expression of p27^{KIP1} was not significantly affected by TSA. These results indicate that expression of p21^{WAF1} in osteoclasts is specifically increased by TSA.

Knockdown of p21^{WAF1} suppresses TSA-induced apoptosis of osteoclasts

RNAi experiments were conducted to address the role of TSA-induced upregulation of p21^{WAF1} in osteoclast apoptosis. Primary bone-marrow-derived cells were infected with the lentiviral shRNA vectors. First, the effectiveness of the sh-21^{WAF1}-knockdown was examined, with sh-LacZ as the control. Infection with p21^{WAF1}-shRNA-expressing virus was performed simultaneously with RANKL treatment. Three days after infection, the cells were treated with TSA for 24 h, collected, and subjected to western blotting for p21^{WAF1}. This confirmed that sh-p21^{WAF1} effectively suppressed the p21^{WAF1} protein (Figure 4A). To examine the effect of TSA-induced p21^{WAF1} on mature osteoclasts, infection with lentiviral shRNAs was performed 2 days after the addition of RANKL. One day after infection, the cells were treated with TSA for 24 h, followed by TRAP staining. In the cells infected with sh-p21^{WAF1}, the TSA-induced reduction in TRAP-positive MNCs was inhibited, as compared with the TSA-induced reduction in TRAP-positive MNCs among cells infected with sh-LacZ. At 100 nM of TSA, TRAP-positive MNCs among the sh-p21^{WAF1}-infected cells were reduced by 38%, compared to a 64% reduction in the sh-LacZ-infected cells (Figure 4B). Flow cytometry with Annexin V staining also showed that the suppression of p21^{WAF1} significantly reduced the TSA-directed apoptosis of osteoclasts, although residual apoptosis occurred (Figure 4C). From these findings, we concluded that the reduction in TSA-directed apoptosis was primarily due to the suppression of p21^{WAF1} upregulation. Taken together, these RNAi experiments clearly demonstrated that aberrant TSA-induced upregulation of p21^{WAF1} could mediate TSA-directed osteoclast apoptosis.

TSA inhibits RANKL-directed bone destruction *in vivo*

To examine the effect of TSA *in vivo*, we locally administered RANKL or RANKL plus TSA in colla-

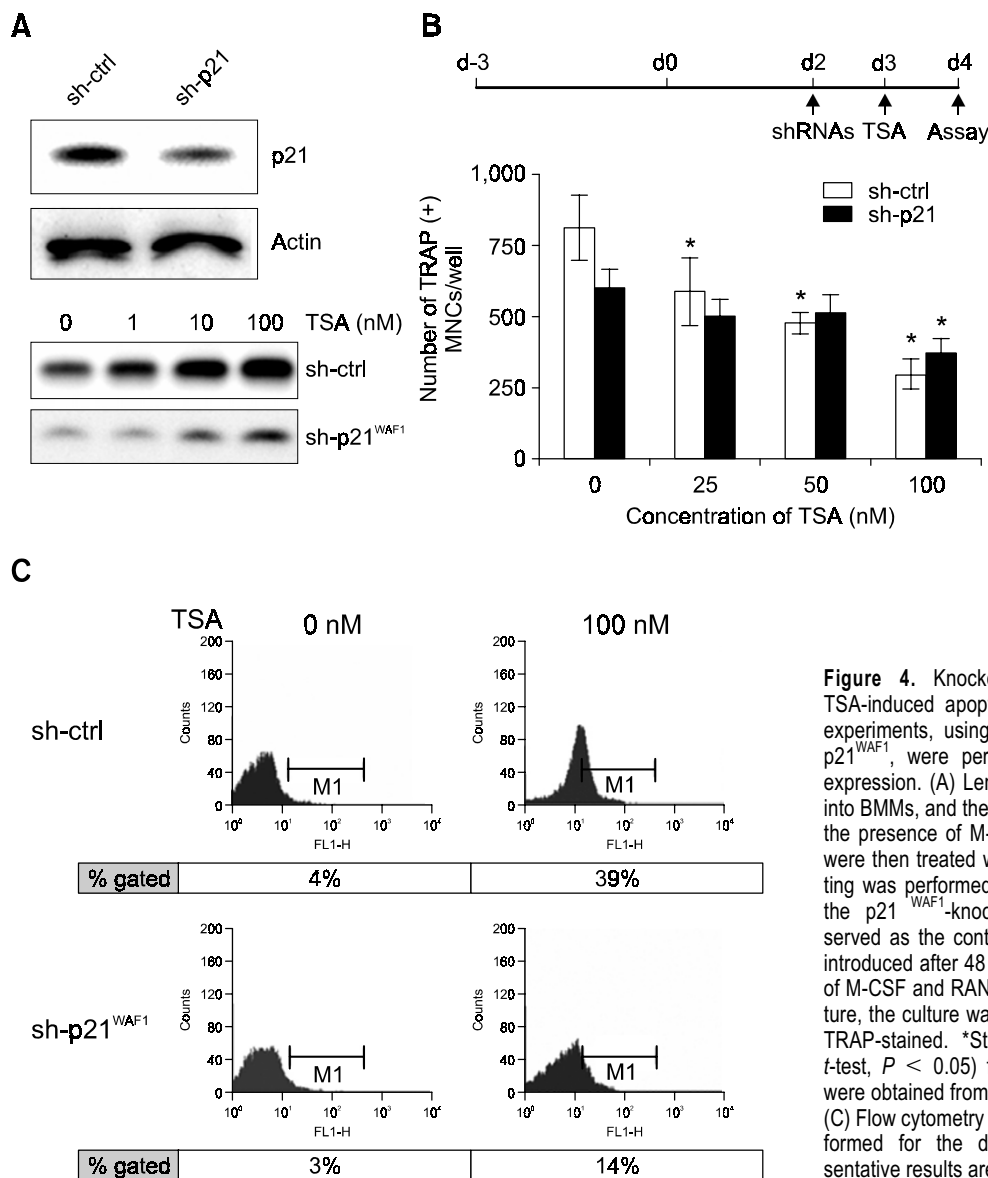


Figure 4. Knockdown of p21^{WAF1} suppresses TSA-induced apoptosis of osteoclasts. The RNAi experiments, using lentiviral shRNA that targeted p21^{WAF1}, were performed to knockdown p21^{WAF1} expression. (A) Lentiviral shRNAs were introduced into BMMs, and the cells were cultured for 3 days in the presence of M-CSF and RANKL. The cultures were then treated with TSA for 24 h. Western blotting was performed to confirm the effectiveness of the p21^{WAF1}-knockdown. sh-LacZ-infected cells served as the control. (B) Lentiviral shRNAs were introduced after 48 h of cell culture in the presence of M-CSF and RANKL. After an additional 24 h-culture, the culture was treated with TSA for 24 h and TRAP-stained. *Statistically significant (Student's *t*-test, *P* < 0.05) from none TSA. Similar results were obtained from three independent experiments. (C) Flow cytometry with Annexin V staining was performed for the detection of apoptosis. Representative results are shown.

gen sponges to mouse calvaria. RANKL treatment caused substantial bone resorption, resulting in the destruction of diploë around the sagittal suture (Figure 5A, D and F). It was evident that the addition of TSA protected the bone from RANKL-directed destruction (Figure 5B and E). The fibrous tissues in the suture had large numbers of spindle-shaped, healthy-appearing cells, implying that the fibroblastic and osteoblastic cells were largely unaffected by the cytotoxic effects of TSA. The bone volume around the suture area, as determined by μ CT, was significantly higher in mice treated with TSA than in those treated with RANKL alone (Figure 5C). TRAP staining clearly showed the reduction of osteoclasts on TSA treatment (Figure 5F-H), supporting that larger

bone volume involves inhibitory effect of TSA on osteoclast. Recently, it was reported that HDAC inhibitors promote osteoblast differentiation (Schroeder and Westendorf, 2005; Jeon *et al.*, 2006). Considering these reports, promoting effect of TSA on osteoblasts also contributes to the bone volumes. Since we placed the TSA-loaded collagen sponge only for 2 days in this study, it was not considered that enhanced osteoblast activity largely affected the bone volume within 2 days. However, on the prolonged treatment for 7 days, we could observe an increase of bone matrix in H-E sections (data not shown). These *in vivo* features indicated that locally delivered TSA could inhibit RANKL-directed bone destruction.

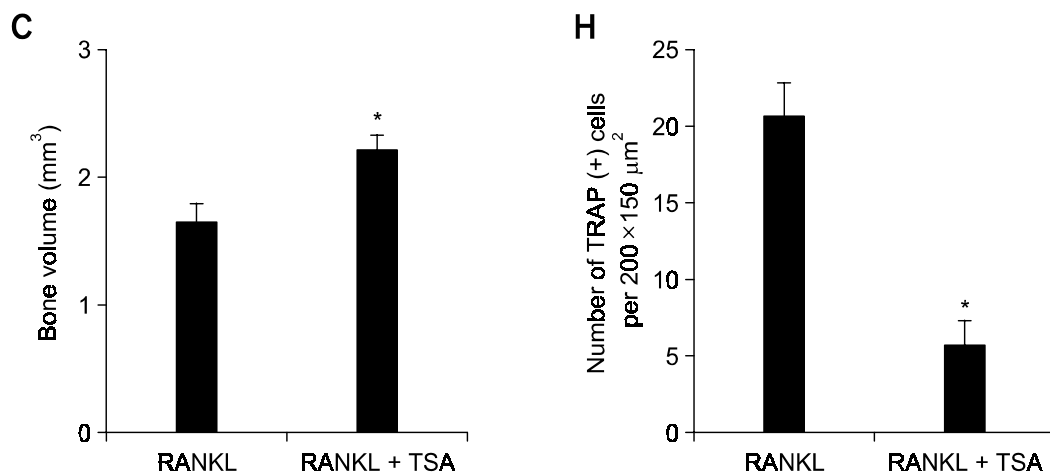
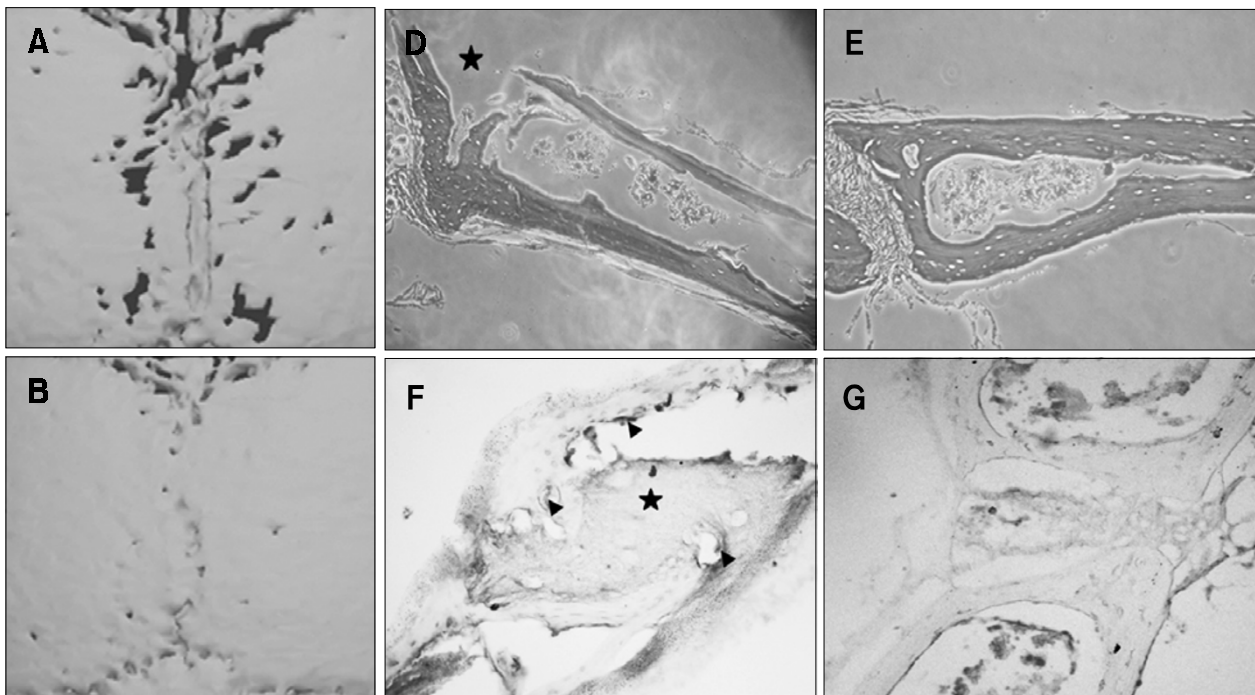


Figure 5. TSA inhibits RANKL-directed bone destruction *in vivo*. Collagen sponges soaked with RANKL or RANKL plus TSA were placed on the center of sagittal suture on the calvaria. After 2 days of treatment, calvariae were collected and analyzed by μ CT (A-C) and histology with H-E staining (D, E) and TRAP staining (F-H). Reconstructed μ CT views of calvariae treated with RANKL and RANKL plus TSA are shown in (A) and (B), respectively. Bone volumes were measured from four animals per group by μ CT in the regions shown in A and B (C). H-E staining views of RANKL (D) and RANKL plus TSA (E). TRAP staining views of RANKL (F) and RANKL plus TSA (G). Number of TRAP(+) cells attached on bone surface were counted in 4 mm-wide area along the sagittal suture (H). The stars in D and F indicate disruption of diploë, and the arrow heads in F indicate TRAP(+) osteoclasts which were counted. Data are averages \pm SDs ($n = 4$). *Statistically significant (Student's *t*-test, $P < 0.05$).

Discussion

This study demonstrates a novel action of TSA—the induction of apoptosis in mature osteoclasts. Previously, Rahman *et al.* (2003) reported that HDIs,

TSA and sodium butyrate, suppressed differentiation of BMCs into osteoclasts. Their study focused on the effects of HDIs on osteoclastogenesis. BMCs from the rat and mouse and RAW-D cell line were treated with HDIs during the osteoclastic differentiation. The

HDI were shown to reduce the formation of osteoclast precursor cells and to inhibit the fusion of osteoclast precursors. Although this same group reported on the mechanism by which HDIs inhibit osteoclastogenesis (Nakamura *et al.*, 2005), there are few reports on the effects of HDIs on mature osteoclasts. Herein, we prepared primary mature osteoclasts by culturing mouse BMCs in the presence of RANKL and other cytokines for 3 days. Subsequently, the cells were treated with TSA in the presence of RANKL for one day. We observed an increase in the number of Annexin V-positive cells in a dose-dependent manner and the activation of caspases-3 and -9 (Figure 2). These results provide strong evidence that TSA directs mature osteoclasts to apoptotic cell death. As mentioned above, the apoptosis of mature osteoclasts has practical significance (Hughes *et al.*, 1996; Luckman *et al.*, 1998; Weinstein and Manolagas, 2000). Thus, our findings strongly support HDIs as potential therapeutic agents for conditions involving excessive bone resorption.

We have also demonstrated that the upregulation of p21^{WAF1} contributes to TSA-induced osteoclast apoptosis. Numerous reports have identified p21^{WAF1} as a protein that is induced primarily by HDIs. p21^{WAF1} is a multi-functional protein (Coqueret, 2003) and it is well-known that p21^{WAF1} negatively modulates cell-cycle progression. In addition to regulating the cell cycle, many studies suggest that p21^{WAF1} plays important roles in protecting cells from caspase-dependent apoptosis (Gartel and Tyner, 2002; Liu *et al.*, 2003; Chopin *et al.*, 2004). However, paradoxically, in some cases p21^{WAF1} can promote apoptosis, while the mechanism by which p21^{WAF1} exerts osteoclast apoptosis remains to be found (Burgess *et al.*, 2001; Gartel and Tyner, 2002; Liu *et al.*, 2003). In our study, TSA induced upregulation of p21^{WAF1} in a dose-dependent manner and as early as 3 h after treatment (Figure 3). Infection with sh-p21^{WAF1}-expressing lentivirus shows that the knockdown of p21^{WAF1} profoundly reduces the number of Annexin V-positive cells on the treatment with TSA (Figure 4), indicating that suppression of p21^{WAF1} inhibits TSA-directed apoptosis of osteoclasts. We observed the activation of caspase 3 in sh-p21^{WAF1}-infected osteoclasts still occurred by TSA (data not shown). Considering that knockdown of p21^{WAF1} partly rescued TSA-induced apoptosis, this suggests that the aberrant upregulation of p21^{WAF1}-induced apoptosis may involve a caspase-independent pathway. In addition, it has been suggested that p21^{WAF1} plays a role during osteoclast differentiation (Okahashi *et al.*, 2001; Sankar *et al.*, 2004) and, sh-p21^{WAF1} may affect differentiation. Thus, we infected the cells on third day after RANKL-treatment (Figure 4). It was also checked the occurrence of

TSA-induced apoptosis in osteoclasts at day 3, and confirmed that TSA-induced the apoptosis (data not shown). However, we cannot totally exclude the possibility that the effect of sh-p21^{WAF1} on osteoclast differentiation affects TSA-induced apoptosis. Collectively, our results suggest that the aberrant upregulation of p21^{WAF1} contributes to TSA-induced apoptosis of mature osteoclasts.

Lastly, we examined the feasibility of HDIs for potential use in therapies for excessive bone resorption. Local delivery of TSA to animals was preferred due to the potential cytotoxic effects of HDIs on systemic administration. We showed that addition of TSA reduces osteoclasts and inhibits bone destruction (Figure 5). These features strongly support that TSA profoundly inhibits RANKL-directed bone destruction, consistent with the *in vitro* results. Both the inhibition of osteoclastogenesis and the induction of osteoclast apoptosis may result in this inhibition of bone destruction *in vivo*. It has recently been reported that the HDI FR901228 in systemic circulation inhibits bone destruction in a model of adjuvant-induced arthritis (Nakamura *et al.*, 2005). In addition, it was also reported that HDIs increase bone formation in an organ culture of mouse calvaria (Jeon *et al.*, 2006). Even though it was not considered that enhanced osteoblast activity largely affected the bone volume within 2 days, we could observe that the treatment prolonged for 7 days resulted in increased bone matrix. These data, coupled with our findings, strongly suggest that HDIs may be suitable candidates for treating bone disease.

Acknowledgement

The authors wish to acknowledge the financial support from Korea Research Foundation (KRF-2005-015-E00214: KMW), and Korea Health 21 R&D Project, Ministry of Health and Welfare (00044975 : KMW).

References

- Boyle WJ, Simonet WS, Lacey DL. Osteoclast differentiation and activation. *Nature* 2003;423:337-42
- Burgess AJ, Pavey S, Warrener R, Hunter LJ, Piva TJ, Musgrove EA, Saunders N, Parsons PG, Gabrielli BG. Up-regulation of p21 (WAF1/CIP1) by histone deacetylase inhibitors reduces their cytotoxicity. *Mol Pharmacol* 2001;60: 828-37
- Chopin V, Slomianny C, Hondermarck H, Le Bourhis X. Synergistic induction of apoptosis in breast cancer cells by cotreatment with butyrate and TNF-alpha, TRAIL, or anti-Fas agonist antibody involves enhancement of death receptors' signaling and requires P21 (waf1). *Exp Cell Res* 2004;298: 560-73

- Coqueret O. New roles for p21 and p27 cell-cycle inhibitors: a function for each cell compartment? *Trends Cell Biol* 2003;13:65-70
- Fuller K, Lean JM, Bayley KE, Wani MR, Chambers TJ. A role for TGFbeta (1) in osteoclast differentiation and survival. *J Cell Sci* 2000;113:2445-53
- Gartel AL, Tyner AL. The role of the cyclin-dependent kinase inhibitor p21 in apoptosis. *Mol Cancer Ther* 2002;1:639-49
- Gui CY, Ngo L, Xu WS, Richon VM, Marks PA. Histone deacetylase (HDAC) inhibitor activation of p21WAF1 involves changes in promoter-associated proteins, including HDAC1. *Proc Natl Acad Sci USA* 2004;101:1241-6
- Hughes DE, Dai A, Tiffée JC, Li HH, Mundy GR, Boyce BF. Estrogen promotes apoptosis of murine osteoclasts mediated by TGF-beta. *Nat Med* 1996;2:1132-6
- Jeon EJ, Lee KY, Choi NS, Lee MH, Kim HN, Jin YH, Ryoo HM, Choi JY, Yoshida M, Nishino N, Oh BC, Lee KS, Lee YH, Bae SC. Bone morphogenetic protein-2 stimulates Runx2 acetylation. *J Biol Chem* 2006;281:16502-11
- Kim HJ, Chang EJ, Kim HM, Lee SB, Kim HD, Kim SG, Kim HH. Antioxidant alpha-lipoic acid inhibits osteoclast differentiation by reducing nuclear factor-kappaB DNA binding and prevents *in vivo* bone resorption induced by receptor activator of nuclear factor-kappaB ligand and tumor necrosis factor-alpha. *Free Radic Biol Med* 2006;40:1483-93
- Liu S, Bishop WR, Liu M. Differential effects of cell cycle regulatory protein p21 (WAF1/Cip1) on apoptosis and sensitivity to cancer chemotherapy. *Drug Resist Updat* 2003;6:183-95
- Luckman SP, Coxon FP, Ebetino FH, Russell RG, Rogers MJ. Heterocycle-containing bisphosphonates cause apoptosis and inhibit bone resorption by preventing protein prenylation: evidence from structure-activity relationships in J774 macrophages. *J Bone Miner Res* 1998;13:1668-78
- Marks PA, Richon VM, Rifkind RA. Histone deacetylase inhibitors: inducers of differentiation or apoptosis of transformed cells. *J Natl Cancer Inst* 2000;92:1210-6
- Nakamura T, Kukita T, Shobuike T, Nagata K, Wu Z, Ogawa K, Hotokebuchi T, Kohashi O, Kukita A. Inhibition of histone deacetylase suppresses osteoclastogenesis and bone destruction by inducing IFN-beta production. *J Immunol* 2005;175:5809-16
- Okahashi N, Murase Y, Koseki T, Sato T, Yamato K, Nishihara T. Osteoclast differentiation is associated with transient upregulation of cyclin-dependent kinase inhibitors p21 (WAF1/CIP1) and p27 (KIP1). *J Cell Biochem* 2001;80:339-45
- Piekarz R, Bates S. A review of depsipeptide and other histone deacetylase inhibitors in clinical trials. *Curr Pharm Des* 2004;10:2289-98
- Rahman MM, Kukita A, Kukita T, Shobuike T, Nakamura T, Kohashi O. Two histone deacetylase inhibitors, trichostatin A and sodium butyrate, suppress differentiation into osteoclasts but not into macrophages. *Blood* 2003;101:3451-9
- Sankar U, Patel K, Rosol TJ, Ostrowski MC. RANKL coordinates cell cycle withdrawal and differentiation in osteoclasts through the cyclin-dependent kinase inhibitors p27KIP1 and p21CIP1. *J Bone Miner Res* 2004;19:1339-48
- Schroeder TM, Westendorf JJ. Histone deacetylase inhibitors promote osteoblast maturation. *J Bone Miner Res* 2005;20:2254-63
- Weinstein RS, Manolagas SC. Apoptosis and osteoporosis. *Am J Med* 2000;108:153-64
- Wolffe AP, Hayes JJ. Chromatin disruption and modification. *Nucleic Acids Res* 1999;27:711-20
- Yi T, Kim HJ, Cho JY, Woo KM, Ryoo HM, Kim GS, Baek JH. Tetraspanin CD9 regulates osteoclastogenesis via regulation of p44/42 MAPK activity. *Biochem Biophys Res Commun* 2006;347:178-84